Design and characterization of a lightweight and flexible carbon fiber-loaded silicone foam-based broadband metamaterial absorber for microwave applications

Hanadi Breiss, Aicha El Assal, Ratiba Benzerga, Ali Harmouch, Akil Jrad, Ala Sharaiha

▶ **To cite this version:**

Hanadi Breiss, Aicha El Assal, Ratiba Benzerga, Ali Harmouch, Akil Jrad, et al.. Design and characterization of a lightweight and flexible carbon fiber-loaded silicone foam-based broadband metamaterial absorber for microwave applications. Materials Research Bulletin, 2024, 176, pp.112791. 10.1016/j.materresbull.2024.112791 . hal-04566376

HAL Id: hal-04566376
https://hal.science/hal-04566376v1

Submitted on 30 May 2024

HAL is a multi-disciplinary open access archive for the deposit and dissemination of scientific research documents, whether they are published or not. The documents may come from teaching and research institutions in France or abroad, or from public or private research centers.

L'archive ouverte pluridisciplinaire **HAL**, est destinée au dépôt et à la diffusion de documents scientifiques de niveau recherche, publiés ou non, émanant des établissements d'enseignement et de recherche français ou étrangers, des laboratoires publics ou privés.

Distributed under a Creative Commons Attribution - NonCommercial 4.0 International License

Journal Pre-proof

Highlights

- Simple fabrication of a metamaterial absorber based on organic compound;
- Elaboration of silicone foam using a Particle-Template method and sugar crystals;
- Use of long carbon fibers (12mm) for broadband absorption performance;
- Absorption bandwidth between 4 and 18 GHz with a total absorber thickness of 16 mm;

ACCEPTED MANUSCRIPT / CLEAN COPY

Journal Pre-proof

Design and Characterization of a Lightweight and Flexible Carbon Fiber-Loaded Silicone Foam-Based Broadband Metamaterial Absorber for Microwave Applications

Hanadi Breiss[1,2], Aicha El Assal[1,2], Ratiba Benzerga[1,*], Ali Harmouch[2], Akil Jrad[2] and Ala Sharaiha[1]

1. Univ Rennes, CNRS, IETR-UMR 6164, Rennes, France

2. Lebanese University, Faculty of Sciences and Faculty of Engineering, Tripoli, Lebanon

* Corresponding author: ratiba.benzerga@univ-rennes.fr

Abstract

This study reports a simple fabrication technique for creating a flexible, organic, and microwave-absorbing material using carbon fiber-loaded silicone foam. The "particle-template" elaboration method, using sugar crystals as sacrificial particles, is conducted. The material's density is adjusted by varying the sugar crystal concentration while ensuring effective dispersion of carbon fibers in the silicone foam matrix. The dielectric characterization of a composite with a density of 0.33g/cm³ and loaded with 2 wt.% of 12mm carbon fibers results in a permittivity ranging from 7 to 1.1 and a dielectric loss ranging from 1.9 to 0.7 across the frequency range of 2-18 GHz. These properties are used in a parametric study to optimize the overall dimensions size of a structured absorber to achieve wideband absorption performance. The resulting prototype, with a total thickness of 16 mm, demonstrates promising performance by exhibiting broadband absorption (4-18 GHz), as predicted by simulation.

KEYWORDS: A. composites, A. organic compounds, D. dielectric properties.

ACCEPTED MANUSCRIPT / CLEAN COPY

Journal Pre-proof

1. Introduction

The presence of electromagnetic (EM) waves, including radio waves, is pervasive in our modern world, serving various practical applications [1–3]. However, these waves can interfere with the proper functioning of sensitive systems like electronic devices [4–6]. Hence, it is important to have control over the propagation or absorption of EM waves to ensure their effective utilization.

In recent years, the demand for EM absorber materials with increasingly stringent specifications has been on the rise. These materials need to satisfy specific requirements, such as being lightweight, thin, flexible, and capable of efficiently absorbing and dissipating EM waves across a broad frequency range [7,8]. As detection systems and electromagnetic equipment encompass wider frequency ranges, the need for radar-absorbing materials with robust and broadband absorption capabilities becomes increasingly vital.

Composite material-based absorbers, have gained significant attention in the field due to their lightweight nature, cost-effectiveness, and ability to absorb a wide range of frequencies [9,10]. These absorbers typically consist of a dielectric matrix, such as polyethylene terephthalate (PET) [11], polyurethane (PU) [12] or epoxy [13–15], combined with lossy loads, such as conductive [16] or dielectric particles [17,18]. Efforts to optimize absorption performance have focused on designing structures like pyramidal [19,20] and multilayer [21,22] structures based on the principle of impedance matching. However, these structures often require significantly large thickness, particularly for low-frequency absorption (such as L and S bands or UHF range), limiting their practical applications and necessitating further improvement. To address this, attempts have been made to enhance low-frequency absorption without increasing the thickness of the absorbing materials [22–24]. In our previous work, we demonstrated that using longer carbon fibers (CFs), such as those measuring 12 mm in length, improves low-frequency absorption [23,24].

ACCEPTED MANUSCRIPT / CLEAN COPY

For several years, metamaterials have been the subject of extensive research as electromagnetic (EM) absorbers [25]. These materials are artificial and have unusual electromagnetic properties not found in naturally occurring materials. Typically, metamaterials consist of a metallic layer with periodic structures on a dielectric substrate, which is further metalized on the backside. By designing specific patterns on the metallic layer, they can effectively absorb a targeted range of EM wavelengths. Initially developed for narrowband absorption, these artificial absorbers have made significant advancements in their capability to absorb microwaves across a wide frequency range [26], The evolution of metamaterial-based absorbers has allowed for their expanded applications, surpassing the limitations of their initial narrowband usage [27].

Over the last decade, significant progress in developing metamaterials with broadband absorption capabilities has been made, and this, using different approaches or principles. The first successful approach consists of the use of the same resonant structure shape, such as split-ring resonators or loop resonators, but with different dimensions. By combining these different structures which resonate at different frequencies, Nguyen and al., have been able to create a metamaterial with a broadband absorption performance (S_{11} < -10 dB) between 10.5 and 12.7 GHz [28]. Another approach consists of the stacking, along length, of several resonant structures to result in multilayer [29] or 3D [30] metamaterial absorbers. In this manner, broadband absorption has been obtained, between 10 GHz and 30 GHz, by Sun and al. [29], and between 8 GHz and 14 GHz, by Ding and al. [30]. Furthermore, several studies have focused on the association of passive elements (such as resistors) with metamaterial structures to broaden their operating band [31]. For example, Nguyen et al. [31] proposed adding 4 resistors to a ring structure, which allows the broadening of the absorption bandwidth from 0.2 GHz (between 12.4 and 12.6 GHz) to 4.8 GHz (between 7.8 and 12.6 GHz). More recently, and in our previous work [32], by combining metamaterials with a thin layer of lossy material (epoxy foam loaded with 0.075 wt.% of CFs), it was possible to move from

ACCEPTED MANUSCRIPT / CLEAN COPY

a multi-resonant absorber to a broadband absorber with S_{11} < -10 dB between 2.7 GHz and 18 GHz, and with a total thickness of only 16.2 mm. However, all these metamaterial-based absorbers are rigid, due to the use of rigid dielectric substrates, which make them not suitable for use in flexible or conformal structures such as wearable devices or flexible displays. For this reason, some recent studies have been focused on the use of flexible substrates to achieve flexible metamaterial absorbers [33]. Nevertheless, there still remains another inconvenience to overcome, the low corrosion resistivity, due to the use of a metallic layer for these metamaterial structures.

Recently, absorbers with a periodic structure exclusively made of composite materials have been studied. For example, Epoxy resin loaded with magnetic metallic particles [34] or reduced graphene oxide loaded polypropylene fabrics [35], have been proposed. These materials have shown very interesting absorption results over a wide frequency range for relatively small thicknesses. However, the design and optimization of flexible broadband EM absorbers remains a challenge due to the multitude of possibilities that open up, particularly from the point of view of their composition (choice of matrix and charge) and of their geometry, to produce absorber materials that present increasingly thin, lightweight and ideally easy to produce.

This study aims to propose a straightforward approach for fabricating an organic metamaterial absorber with a broadband absorption performance using silicone foam loaded with carbon fibers. On the one hand, The fabrication method employed is the Particle-template method [36], a simple technique involving the mixing of a sacrificial filler with the desired matrix, followed by the removal of the filler to create a porous material. Various combinations of matrix and sacrificial fillers have been explored in previous literature [36–38]. For instance, in [38], hollow microspheres were utilized as a sacrificial filler to produce a Si3N4 ceramic foam. On the other hand, we employ a two-layer structure design strategy inspired by the previous work of Zhang et al. [39] and adapted for the frequency range between 2 and 18 GHz. In this work, by combining the Particle-template

ACCEPTED MANUSCRIPT / CLEAN COPY

method with this simplified design approach, we aim to achieve an effective organic metamaterial absorber with broadband absorption capabilities.

This article is structured as follows: elaboration and characterization methods of the composite are first detailed. Subsequently, the design of the chosen metamaterial structure, as well as the results of the parametric study are shown to explain the dimensions of the final structure. Finally, the microwave absorption performances of the achieved prototype are presented and compared to the simulated performance.

2. Material and methods

2.1. Elaboration method of the absorber composite

The "sacrificial template method" is used to produce silicone foam [36]. In our case, a silicone resin has been used as a matrix with the sugar filler. The elastomeric silicone selected for the fabrication of absorber materials is a two-component system composed of a resin and a hardener, Momentive's RTV615-A resin and RTV615-B hardener, purchased from “Composites Distribution”. The resin and hardener blend exhibits a viscosity of 4000 cps. These two constituents should be combined in a mass ratio of Resin to Hardener of 10:1. Carbon fibers, of 7 µm in diameter and 12 mm in length, acquired from “Apply Carbon”, are employed as absorbing load.

ACCEPTED MANUSCRIPT / CLEAN COPY

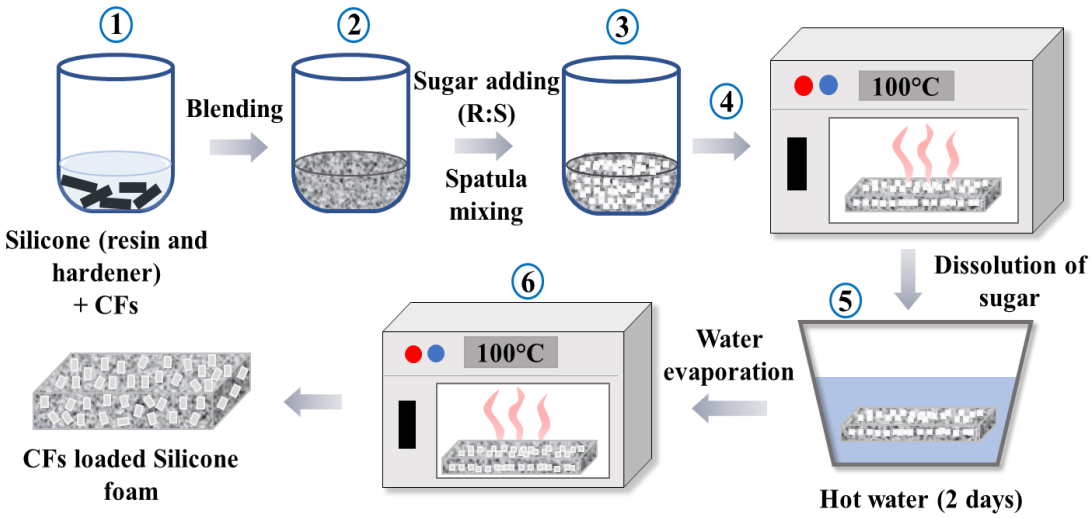

Fig. 1. Elaboration method of the absorber composite based on silicone foam loaded with CFs.

The elaboration process of silicone foams loaded with CFs involves several steps (Fig. 1). First, the CF load are pre-dispersed in a solvent, using an ultrasonic probe (Vibra-Cell from "Sonics") with a power of 300W for 10 minutes. The pre-dispersed filler is then incorporated into a resin / hardener mixture, then the whole is homogenized via spatula mixing for 5 minutes. Next, sugar crystals of around 0.5 mm diameter (between 0.2 and 0.8 mm) are introduced into the CFs/silicone mixture, and mixed again with a spatula for several minutes (~10 minutes), ensuring a homogeneous distribution of sugar crystals and CFs within the blend. The resulting mixture is then molded and placed in an oven at 100°C for at least 2 hours; this step finalizes polymerization and provides definitive mechanical properties to the silicone. Following demolding, the sample undergoes immersion in warm water at 60°C for 1 to 2 days (depending on its size); this step aims to dissolve the sugar crystals. Water is periodically replaced to accelerate this dissolution process. Finally, the sample is replaced in the oven at 100°C for the water evaporation, to obtain a silicone foam loaded with CFs.

ACCEPTED MANUSCRIPT / CLEAN COPY

2.2. Characterization methods

2.2.1. Structural characterization

The morphology of the foam composites was analyzed by a Leica DM 2500 M optical microscope and JSM-IT100; JEOL scanning electron microscope (SEM). Composites densities were calculated according to the following formula: $\rho = \frac{m}{V}$ where m is the weight and V is the volume of the sample.

2.2.2. Dielectric and electromagnetic characterization

The dielectric and the EM characterization of the composites were carried out using the free space method [40]. For this measurement, a sample with dimensions of 15 × 15 × 1 cm^3 was placed inside the anechoic chamber in front of two horn antennas (ETS-Lindgren 3115 model), one transmitter, and one receiver (Fig. 2-a). These antennas operate in the [2-18 GHz] frequency range and were connected to a vector network analyzer (VNA Agilent PNA-L) with a wave power of -8 dBm (0.15 mW). Antennas were placed side by side with a negligible angle of incidence shown in Fig. 2-b. The complex permittivity ($\tilde{\varepsilon} = \varepsilon' - j\varepsilon''$) of the characterized materials was then extracted from the measured reflection coefficients (S_{21}) using the method proposed by Fenner et al. [41]. For this, four measurements (four S_{21} parameters) are needed: the sample alone ($S_{\_21(sample)}$), the sample with a metallic plate ($S_{\_21\ (sample\_metal)}$), the metallic plate alone ($S_{\_21\ (metal)}$), and the environment ($S_{\_21\ (env)}$) as shown in (Fig. 2-c). Then, the reflection coefficients Γ of the material alone (Γ_{sample}) and of the material with a metallic plate (Γ_{sample_metal}) are calculated, using the four measurements, as follows:

$$\Gamma_{sample} = \frac{S_{21}(sample) - S_{21}(env)}{S_{21}(env) - S_{21}(metal)} \quad \text{(eq. 1)}$$

ACCEPTED MANUSCRIPT / CLEAN COPY

$$\Gamma_{sample\_metal} = \frac{S_{21}(sample\_metal) - S_{21}(env)}{S_{21}(env) - S_{21}(metal)} \quad \text{(eq. 2)}$$

For these EM measurement, a distance (d) must be ensured between the antennas and the sample, to satisfy the far field condition (eq. 3), where D is the antenna aperture diameter and λ is the highest measured wavelength (at the lowest measured frequency) [41].

$$d \geq \frac{2D^2}{\lambda} \quad \text{(eq. 3)}$$

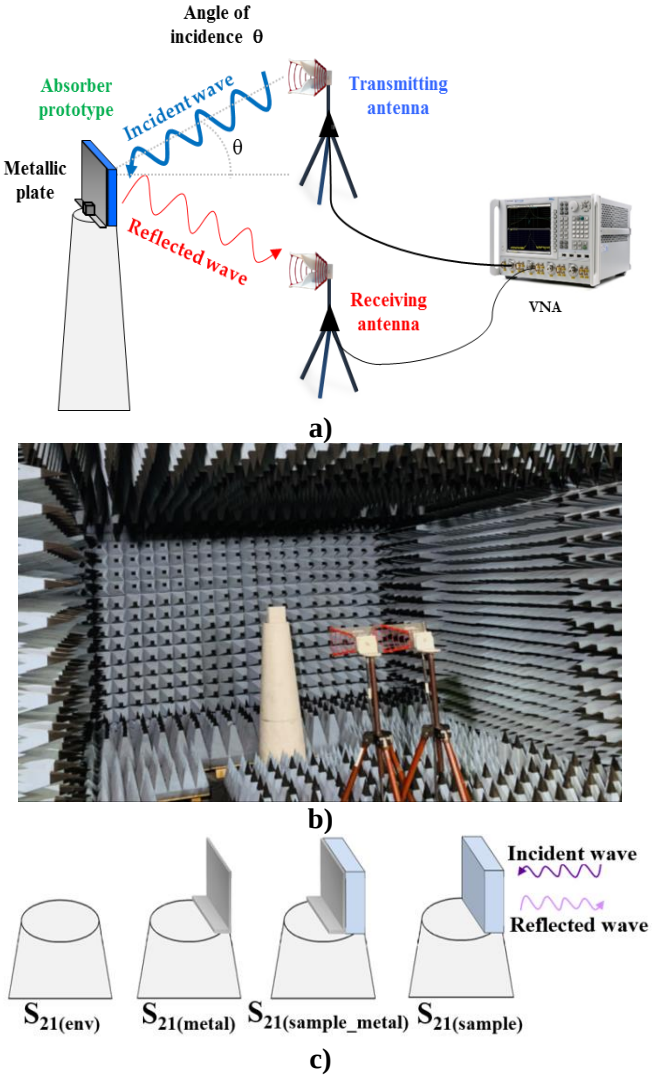

Fig. 2. a) Schematic, **b)** photo of the measurement configuration used for the EM characterization in the anechoic chamber and **c)** different measurements needed for the EM characterization.

ACCEPTED MANUSCRIPT / CLEAN COPY

The measurement of the reflection coefficients of the achieved prototype was performed in the same configuration for the normal incidence (θ = 0 °). An angle of 60° between antennas was used for measurement at oblique incidence of θ = 30°.

2.3. Design and Simulation

The chosen geometry for the organic metamaterial absorber is illustrated in Fig. 3. It consists of a first layer serving as a substrate and a second layer with a periodic "parallelepiped" structure. The choice of this structure, inspired by the work of Zhang et al. [39], was motivated by its ease of implementation.

The simulation of the reflection coefficient of the absorber is carried out using the commercial software CST Microwave Studio, and the measured dielectric properties of the composite material. A Perfect Electric Conductor (PEC) is positioned behind the absorber for this simulation conducted using the frequency domain. In these simulations, the size (surface) used for a single unit is 31 mm x 31 mm. Periodic boundaries are applied to simulate an infinite structure, using the Floquet theory implemented in CST software, in the x and y directions, while the electromagnetic wave propagates along the z-axis. Once the dimensions of the structure are fixed: a (thickness of the first layer), b and c (side and thickness of the parallelepiped structures, respectively), the prototype is manufactured and its absorption performance is measured in an anechoic chamber.

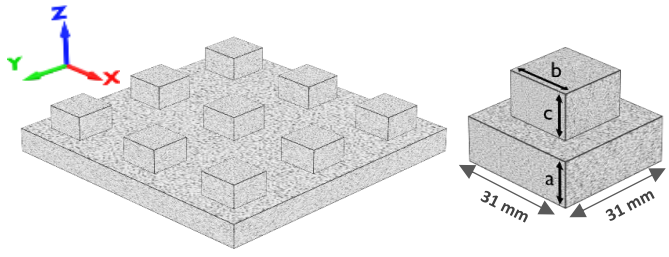

Fig. 3. Chosen design and dimension parameters of the metamaterial structure.

ACCEPTED MANUSCRIPT / CLEAN COPY

For the fabrication of the structured absorber prototype, two layers of CF loaded silicone foam composite are utilized. According to Fig. 4, the first layer is used as a continuous layer while the second one (non-continuous layer) is structured as parallelepiped forms. In our work, these parallelepiped forms are simply cut by scissors. Subsequently, these parallelepipeds are affixed to the first layer by silicone glue. The different dimensions of the chosen structure were obtained after a parametric study which will be presented later in this article (Part 3.3).

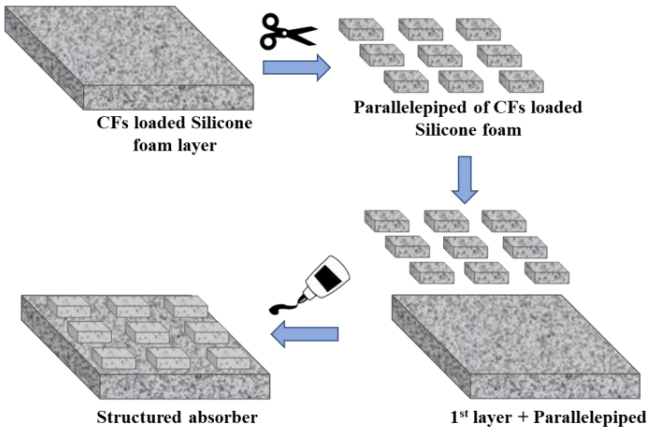

Fig. 4. Fabrication steps of the organic metamaterial absorber prototype based on CF loaded silicone foam composite.

3. Results

3.1. The structure of silicone foams

To investigate the effect of the Resin-to-Sugar (R:S) ratio on silicone foam density and structure, samples without CFs (unloaded silicone foams) were elaborated with eight R:S ratios (1:0, 1:1, 1:2, 1:3, 1:4, 1:5, 1:6, 1:7). Fig. 5 displays photos of achieved samples.

According to this figure, it can be observed that the volume of the samples increases with the amount of added sugar, and their color changes from transparent to whitish, which is due to the multiple reflections of visible light in the increasingly porous structure. The appearance of pores (air bubbles) can also be observed with the naked eye beginning at the ratio of 1:1.

ACCEPTED MANUSCRIPT / CLEAN COPY

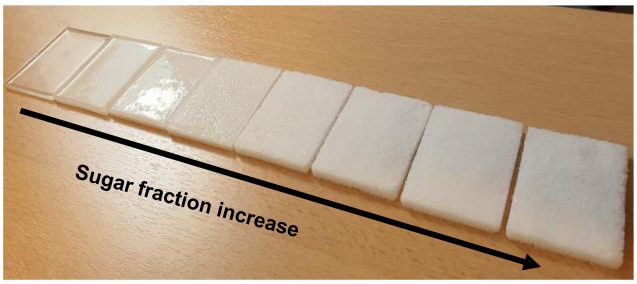

Fig. 5. Photo of silicone foam samples made with different R:S ratios (sugar amount increases from left to right).

These samples were observed using an optical and Scanning electron microscopes. As expected, Fig. 6 illustrates that the number of pores increases with the quantity of sugar added. First, for ratio R:S equal to or lower than 1:2 (Fig. 6-a1 and Fig.6-b1), samples show separated porosities, which are confined inside the resin matrix and so, are only visible by optical observation (thanks to the translucent appearance of the resin). Thus, only some porosities are visible on the surface of the samples, as can be observed by SEM images of the Fig. 6-a2 and Fig.6-b2. In this case, the dissolution of the sugar can be not completed. Secondly, for ratio R:S of 1:3 and 1:4, SEM images Fig. 6-c2 and Fig.6-d2) show an increase of the open porosities towards the sample surface, compared to the lower R:S ratios, which facilitates the dissolving of sugar during the composite elaboration. Finally, for ratio R:S equal to or higher than 1:5 (Fig. 6-e to Fig.6-g), the empty pores (resulting from the dissolution of the sugar) begin to agglomerate (touch each other) to form pores with larger size. With the 1:7 ratio (Fig. 6-g), nearly all the pores cluster together, which can be more easily observed by optical microscope on the zoom of Fig. 6-g'1. This results in a mechanical weakening, making the sample structure very fragile and easy to tear apart.

ACCEPTED MANUSCRIPT / CLEAN COPY

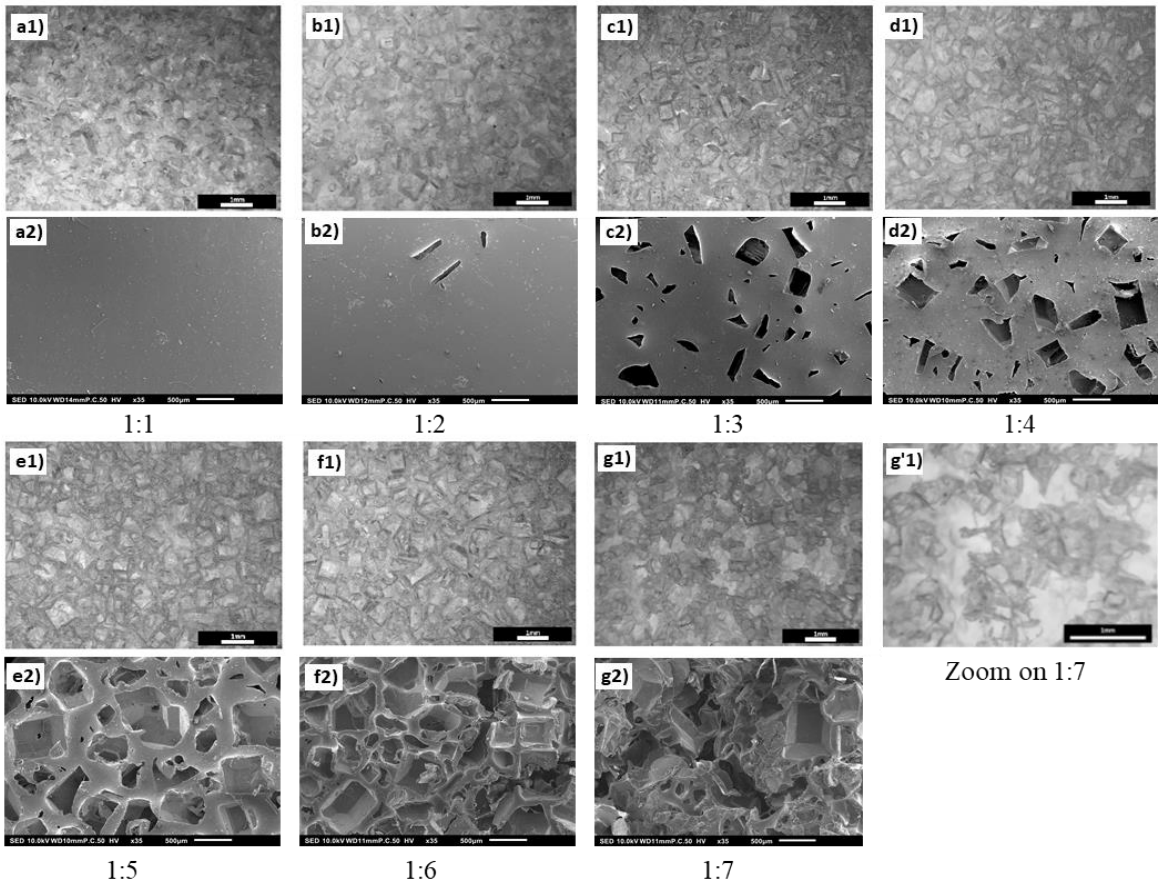

Fig. 6. Optical microscope images (a1 to g'1) and SEM images (a2 to g2) of unloaded silicone foam samples made with different R:S ratios.

Moreover, the expansion of sample volume and the enlargement of pores within these samples foreshadow variations in their density as a function of the amount of added sugar. Density measurements were conducted on these samples, and the results are presented in Table (1). This table illustrates a reduction in sample density as the sugar content increases. For instance, the density decreases from 0.9 $g \cdot cm^{-3}$ for the (1:0) ratio (pure silicone bulk without sugar) to 0.22 $g \cdot cm^{-3}$ for the (1:7) ratio. The size of the porosities, as expected, is between 0.2 and 0.8 mm, which corresponds to the dimensions of the sugar crystals used for the elaboration of these materials.

Table 1. Density values of silicone foam samples elaborated with different R:S ratios.

ACCEPTED MANUSCRIPT / CLEAN COPY

Resin: sugar	1:0	1:1	1:2	1:3	1:4	1:5	1:6	1:7
Density ($g \cdot cm^{-3}$)	0,9	0,7	0,45	0,35	0,32	0,28	0,28	0,22

According to these results, the two ratios (1:3) and (1:4) demonstrate the best compromises between low density and a homogeneous structure while maintaining good mechanical strength. In the case of absorber materials, achieving homogeneity is essential for ensuring that the electromagnetic properties of the absorbers can be reproducible. The introduction of sugar into the resin can potentially disrupt the uniform dispersion of conductive fillers (CFs) within the resin, this is due to the viscosity of the mixture which becomes very high and prevents effective mixing of the blend. So, as the amount of added sugar increases, it becomes increasingly difficult to maintain a consistent distribution of CFs within the resin. This is why we selected a resin-to-sugar ratio of 1:3 when producing the CFs-loaded silicone foams.

3.2. Dielectric properties of silicone foam loaded with 12mm CFs

For this study, a composite based on silicone foam loaded with carbon fibers of 12 mm length were chosen. This choice was motivated by our previous work [23] which showed the interest of long fibers (12 mm) for EM absorption. Here, a resin-to-sugar ratio of 1:3 and 2 wt.% of CFs are used. This choice ensures that our material exhibits high dielectric losses while maintaining a relatively homogeneous and uniform distribution of charges within the material. Fig. 7-a shows the photo of the elaborated composite made with flexible silicone foam loaded with CFs. Fig. 7-b) shows the SEM image of this sample with the CFs stuck in the sample porosities.

To carry out the simulation and parametric study of the structured absorber, dielectric properties of our composite are needed. Fig. 7-c) displays the real permittivity (ε') and dielectric losses ($\tan \delta$) extracted for this sample from measurements in an anechoic chamber. The graph illustrates that both

ACCEPTED MANUSCRIPT / CLEAN COPY

the real permittivity and dielectric losses decrease with increasing frequency. For instance, in the range from 2 GHz to 15 GHz, the real permittivity and dielectric losses decrease from ε' = 7 and tan δ = 1.9 to ε' = 1.1 and tan δ = 0.7.

It should be noted here that usually, for a standard absorber (without structuring) based on a dielectric composite, a low permittivity (as close as possible to that of air ε' ~ 1) associated with high losses, but less than 1, is needed. These conditions are necessary to ensure impedance matching, and therefore low reflection, at the air/material interface [23]. In the case of a structured material, this condition is not necessary, and so, the highest losses are sought.

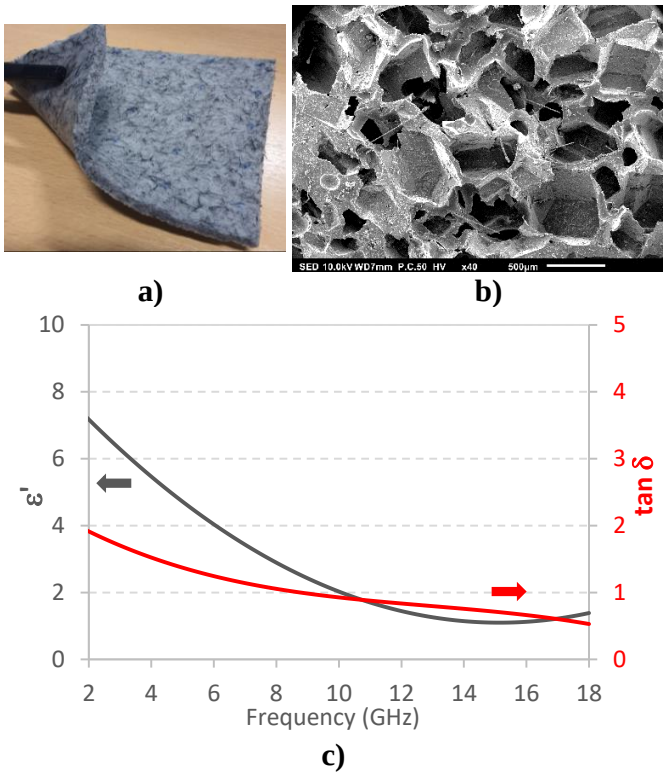

Fig. 7. **a)** Photo of the flexible composite **b)** SEM image of the composite and **c)** Dielectric properties (ε' and tanδ) of the composite based on silicone foam loaded with 2 wt.% of CFs of 12 mm length.

3.3. Simulation of metamaterial absorber based on silicone foam loaded with CFs :

ACCEPTED MANUSCRIPT / CLEAN COPY

The measured properties of CF loaded silicone foam, obtained through measurements conducted in an anechoic chamber, serve as the basis for a parametric study. This study aims to evaluate the impact of each dimension parameter on the absorption performance of the structured organic absorber. In the simulation, the size of the individual unit (period length) is fixed at 31 mm, while the parametric investigation focuses on three variable parameters: a, b, and c. Notably, the structured component, which constitutes the second layer, is a rectangular parallelepiped with 90° angles. It features a square top surface with dimensions b x b and a thickness of c; the thickness of the first layer is a. Limits are imposed on these parameters as follows: the thickness of the first layer (a) varies between 4 and 10 mm, the side length of the square (b) ranges from 10 to 22 mm, and the thickness of the second layer (c) is constrained between 6 and 12 mm. A 1 mm step increment is used for the thicknesses of the two layers (a and c) where a 2 mm increment is applied for the square side length (b). These parameter limits and steps are summarized in Table 2. One can note here that all the simulations done for the parametric study are done for a normal incidence ($\theta = 0°$) of EM waves.

Table 2. Dimension limits and steps used for the parametric study of the metamaterial structure.

Parameters	Min (mm)	Max (mm)	step (mm)
a	4	10	1
b	10	22	2
c	6	12	1

First, Fig.8-a displays the reflection coefficients resulting from the parametric study of the structured absorber, considering different values of a thickness (a) between 4 and 10 mm, to investigate how the thickness of the first layer (a) affects the reflection coefficient of the absorber. The other parameters are fixed to values of b = 12 mm and c = 10 mm. From this first simulation results, we can notice that all the studied structures present an absorption from a frequency around

ACCEPTED MANUSCRIPT / CLEAN COPY

4 GHz. It's also noticeable that as (a) increases from 4 mm to 6 mm, the reflection coefficient decreases. However, beyond a thickness of 7 mm, the absorption coefficient begins to rise once more. The best reflection coefficient is achieved with an optimal thickness of 6 mm; this value is chosen for the rest of the parametric study for the optimization of the other two variables.

Fig. 8-b illustrates the influence of the parallelepiped surface on the reflection coefficient of the periodic structure. It should be noted here that for our simulations, we only considered a square surface (b x b) for the parallelepiped structures. Here, the (b) parameter is varied between 10 and 22 mm and the other parameters are fixed to a = 6 mm and c = 10 mm. The simulation results show that increasing the size of the squares up to 14 mm enhances the absorption of EM waves. However, starting from 16 mm, the absorption peaks shift towards lower frequencies while their absorption level diminishes. For this raison, b = 14 mm was selected because it presents a compromise between absorption at low and high frequencies. It exhibits a prominent resonance peak at 7.8 GHz with a minimum reflection coefficient of -48 dB. Additionally, it provides a wide absorption bandwidth spanning from 3.2 GHz to 18 GHz.

For the last parametric study, values of a = 6 mm and b = 14 mm are kept constant to determine the influence of the second layer thickness (c) on the reflection coefficient; simulation results are presented in Fig. 8-c. Based on these results, a similar trend of the reflection coefficients, as previously obtained when varying the thickness (a) (Fig. 8-a), is observed. As (c) increases from 6 mm to 10 mm, the reflection coefficient decreases. However, when the thickness reaches 11 mm, the absorption coefficient starts to rise again. Thus, the optimal reflection coefficient, the best compromise, is achieved with a thickness of 10 mm. Consequently, the chosen parameters for the prototype are a = 6 mm, b = 14 mm, and c = 10 mm.

ACCEPTED MANUSCRIPT / CLEAN COPY

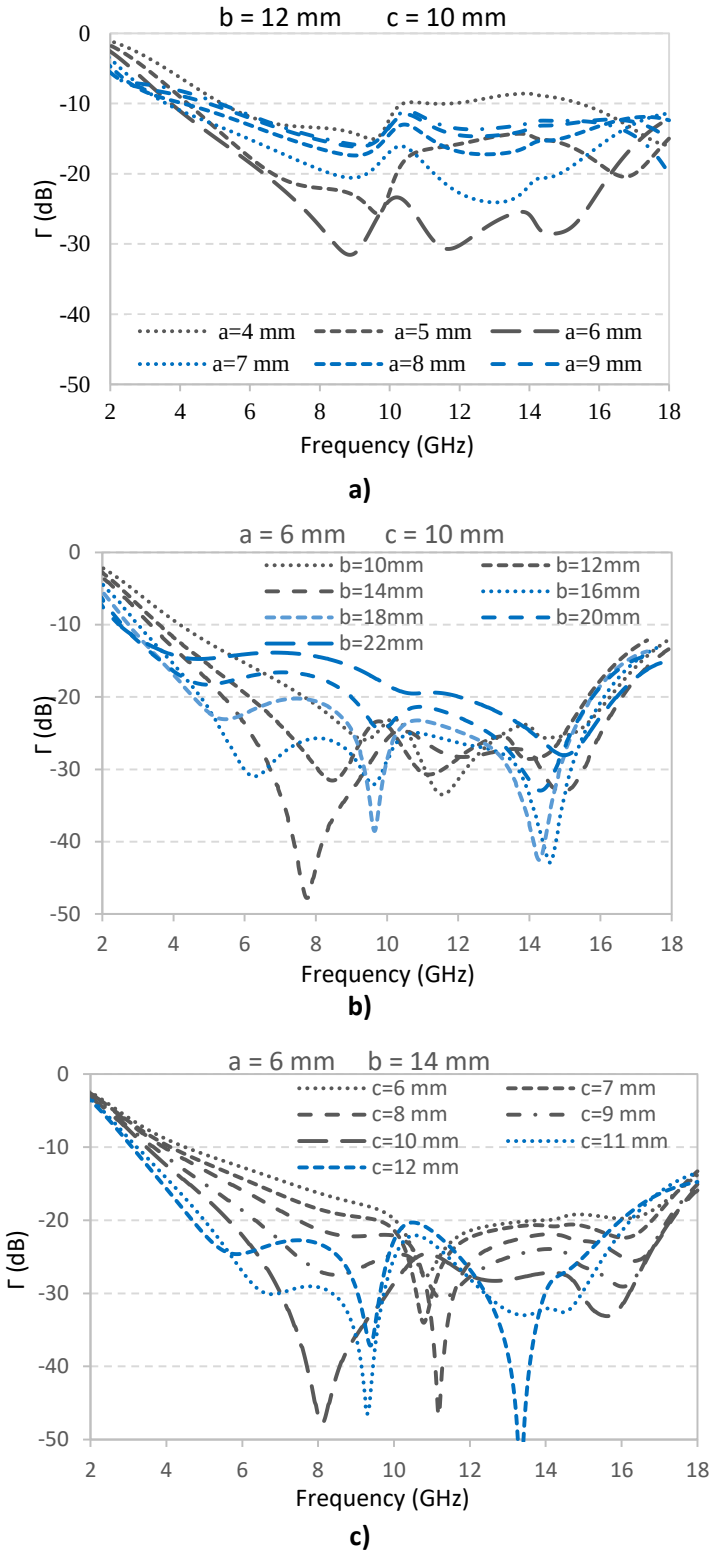

Fig. 8. Simulated reflection coefficients of the organic metamaterial absorber for different values of dimension parameters (a), (b), and (c).

ACCEPTED MANUSCRIPT / CLEAN COPY

It should be noted here that the absorption performance of our structured absorber is mainly related to the different dimensions, and in particular to the thickness of the two layers constituting the absorber. Indeed, the absorption peaks observed in Fig. 8 are a consequence of the resonance frequencies of the two layers of thicknesses (c) and (a + c), as illustrated in Fig. 9. Zhang et al. [39] show that the resonance frequency (*f*) of the periodic structure is dependent on two frequencies, namely, f_1 et f_2, which can be described by the following Lichtenecker formula (eq. 4) [39]:

$$\log f = R_s \log f_1 + (1 - R_s) \log f_2 \qquad \text{(eq. 4)}$$

Where f_1 and f_2 are the resonance frequencies of layers with thicknesses (a + c) and (a), respectively, R_s represents the surface ratio between the upper layer (c) and the lower layer (a); in our case, R_s = $(b/31)^2$.

Fig. 9. Schematic of the periodic structure compared to two monolayers of thickness (a) and thickness (a + c).

3.4. Fabrication and measurement of the structured organic absorber

Fig. 10 displays photographs of the achieved absorber prototype fabricated using a silicone foam loaded with 2 wt.% of 12 mm-CFs. This prototype consists of a first layer of 6 mm thickness, a second layer composed of parallelepiped structures of 10 mm (resulting in a total thickness of 16 mm), and a surface of 14 x 14 mm^2. the distance between the center of each parallelepiped is 31 mm. Dimensions of the final prototype are 150 x 150 x 16 mm^3.

ACCEPTED MANUSCRIPT / CLEAN COPY

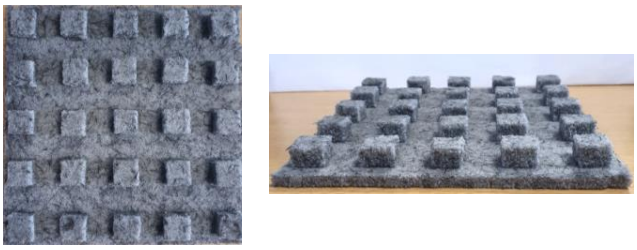

Fig. 10. Photos of the achieved prototype of silicone foam loaded with 2 wt.% of CFs of 12 mm length.

The reflection coefficient Γ of this prototype was measured in an anechoic chamber. To conduct this measurement, the prototype was affixed to a metallic plate of the same surface dimensions (150x150 mm²). Absorption performance was measured in both normal (θ = 0°) and oblique incidence (θ = 30°) of EM waves. The measured absorption performance is compared to the results obtained through simulation in Fig. 11.

Under normal incidence (θ = 0°) as shown in Fig. 11-a, the prototype demonstrates wideband absorption, with a reflection coefficient below -10 dB between 4.2 GHz and 18 GHz and staying below -20 dB between 5.4 GHz and 18 GHz. In the case of oblique incidence (θ = 30°) depicted in Fig. 11-b, the prototype also exhibits broadband absorption spanning from 4 GHz to 18 GHz, with a reflection coefficient below -20 dB between 5.2 GHz and 18 GHz.

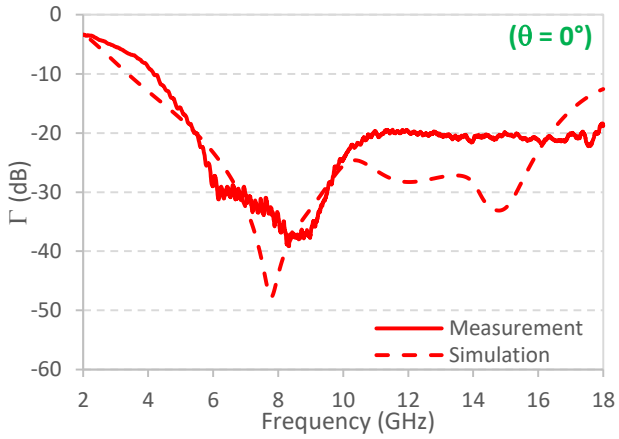

a)

ACCEPTED MANUSCRIPT / CLEAN COPY

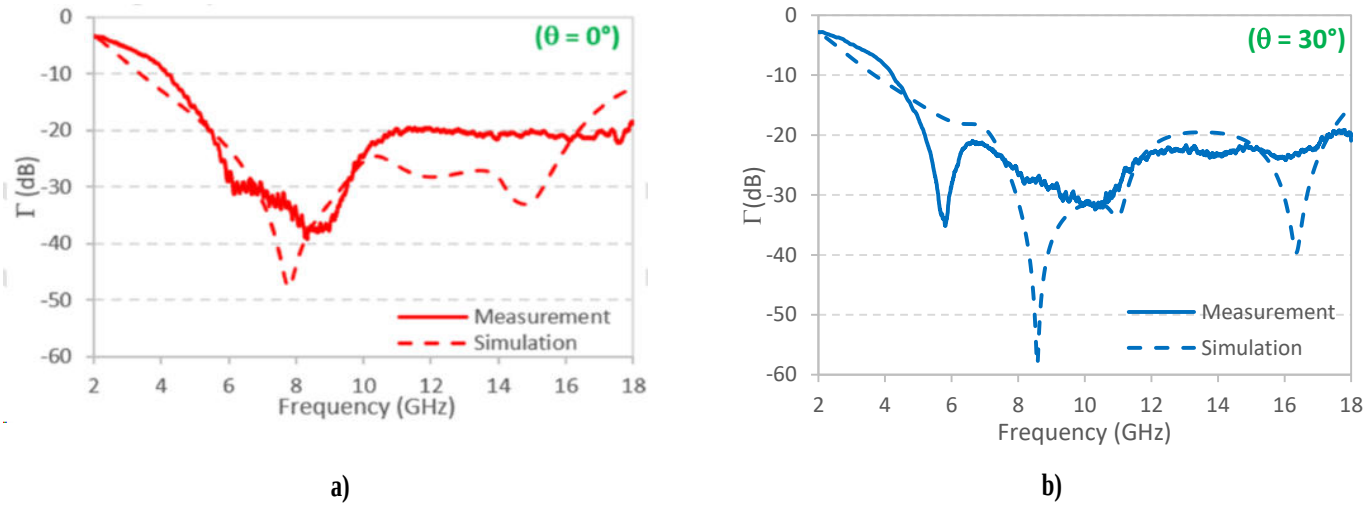

Fig. 11. Simulated and measured reflection coefficients of the prototype for **a)** normal incidence (θ=0°) and **b)** oblique incidence (θ=30°) of EM waves.

Fig. 11 exhibits a good agreement between simulated and measured reflection coefficients for both incidence angles (0° and 30°). The slight variations between these results can be attributed to imperfections in the structure produced by the cutting method of our prototype. Measurement of the dimensions of the produced prototype shows values ranging from 5 to 6 mm for parameter a, between 14 and 16 mm for parameter b, and between 9 and 10 mm for parameter c; as a reminder, the targeted values were a = 6 mm, b = 14 mm, and c = 10 mm.

Fig. 12 illustrates the simulation of the reflection coefficient for the prototype using the selected parameters (a=6 mm, b=14 mm, and c=10 mm) in comparison to three other simulations, each involving a change in one of the parameters (a, b, or c). These simulations provide insight into the tolerance of our prototype's dimensions. Notably, variations in these parameters can impact the absorption level at high frequencies and the magnitude of the absorption peak around 8 GHz. As an example, reducing the thickness of the first layer from 6 mm to 5 mm increases the reflection coefficient from -28 dB to -16 dB at 12 GHz and from -47 dB to -12 dB at 8 GHz.

ACCEPTED MANUSCRIPT / CLEAN COPY

Furthermore, when comparing these simulations to the measurement, we observe that the measured curve falls within the range of the different simulation curves. This confirms that the difference between the simulation and the measurement is primarily due to errors in the molding and cutting of the prototype.

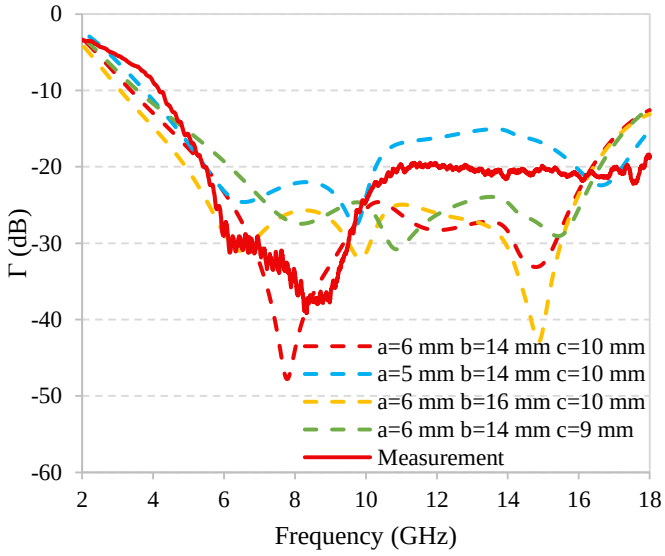

Fig. 12. Measured reflection coefficient of the achieved prototype compared to simulated coefficients made with different values of parameters (a), (b), and (c).

4. Conclusion

Our objective was to introduce a novel microwave-absorbing material that is both flexible and lightweight, achieved through a straightforward fabrication method for the composite and a simplified approach to its structuring. We present the template-particle method, which involves incorporating sugar crystals as sacrificial particles to create silicone foam. The resulting silicon-based composites exhibit varying structures and densities depending on the Resin:Sugar ratio. Among the ratios tested, a ratio of 1:3 was selected as it demonstrated the optimal balance in terms

ACCEPTED MANUSCRIPT / CLEAN COPY

of density, homogeneity, and stable mechanical properties. This ratio allows for a composite density of 0.33 g/cm³, highlighting its suitability for the desired properties of the absorber material.

The dielectric characterization, conducted in the anechoic chamber, of the composite loaded with 2 wt.% of 12mm-CFs, shows high dielectric losses (between 2 and 0.75) associated with a moderate relative permittivity (between 7 and 1.1) in the frequency range of 2-18 GHz. These properties were used for a parametric study to determine the optimal dimensions for a periodic structure, aiming to enhance absorption performance. The chosen design for the absorber combines a first continuous layer of the composite and a second layer composed of parallelepiped structures made with the same composite. The best-simulated reflection coefficient was achieved with a first layer thickness of 6 mm and a structured second layer thickness of 10 mm, the parallelepiped surface is 14 x 14 mm².

A prototype, presenting final dimensions of 16 x 150 x 150 mm^3, was fabricated and measured. A reflection coefficient below -10 dB across the frequency band (4-18) GHz and reaching -20 dB between 5.4 GHz and 18 GHz were then confirmed, thus validating the simulation results.

In conclusion, this study validates the absorption performance of the proposed structured material utilizing carbon fiber loaded silicone foam. The findings suggest that there is potential for enhancing the performance of these silicone foam-based absorbers by exploring more intricate geometries or adjusting the loading percentages of the CFs. These possibilities open up new avenues for the application of this lightweight and flexible absorbing material, paving the way for further advancements in the field.

Acknowledgment

This work is supported by the European Union through European Regional Development Fund (ERDF), Ministry of Higher Education and Research, CNRS, Brittany region, Conseils

ACCEPTED MANUSCRIPT / CLEAN COPY

Journal Pre-proof

Départementaux d'Ille-et-Vilaine and Côtes d'Armor, Rennes Métropole and Saint-Brieuc Armor Agglomération, through the CPER Projects MATECOM and Sophie-Sticc&Ondes. Authors greatly acknowledge Jérôme Sol, Adnan Masri and Ayman Nazih, from IETR, for their technical help.

ACCEPTED MANUSCRIPT / CLEAN COPY

References

[1] I.F. Akyildiz, A. Kak, S. Nie, 6G and Beyond: The Future of Wireless Communications Systems, IEEE Access. 8 (2020) 133995–134030. https://doi.org/10.1109/ACCESS.2020.3010896.

[2] E. Reyes-Vera, D.E. Senior, J.M. Luna-Rivera, F.E. López-Giraldo, Advances in electromagnetic applications and communications, TecnoLógicas. 21 (2018) 9–13. https://doi.org/10.22430/22565337.1052.

[3] H. Lv, Z. Yang, H. Pan, R. Wu, Electromagnetic absorption materials: Current progress and new frontiers, Prog. Mater. Sci. 127 (2022) 100946. https://doi.org/10.1016/j.pmatsci.2022.100946.

[4] R. Redl, Electromagnetic environmental impact of power electronics equipment, Proc. IEEE. 89 (2001) 926–938. https://doi.org/10.1109/5.931490.

[5] M. Hardage, P.D. Henry, Electromagnetic interference (EMI), in: Implant. Defibrillator Ther. Clin. Guide, Springer Science, 2002.

[6] C. Weller, Effects of electromagnetic radiation on equipment, with special reference to protection relays, IEE Colloq. Electromagn. Compat. Electr. Supply Ind. (1990) 4/1-4/3.

[7] M.M. Tirkey, N. Gupta, Electromagnetic absorber design challenges, IEEE Electromagn. Compat. Mag. 8 (2019) 59–65. https://doi.org/10.1109/MEMC.2019.8681370.

[8] M.M. Tirkey, N. Gupta, The quest for perfect electromagnetic absorber: a review, Int. J. Microw. Wirel. Technol. 11 (2019) 151–167. https://doi.org/10.1017/S1759078718001472.

[9] D.D.L. Chung, Composite Materials, Springer London, London, 2010. https://doi.org/10.1007/978-1-84882-831-5.

[10] P. Banerjee, Y. Bhattacharjee, S. Bose, Lightweight Epoxy-Based Composites for EMI Shielding Applications, J. Electron. Mater. 49 (2020) 1702–1720. https://doi.org/10.1007/s11664-019-07687-5.

[11] Z. Lu, L. Ma, J. Tan, H. Wang, X. Ding, Transparent multi-layer graphene/polyethylene terephthalate structures with excellent microwave absorption and electromagnetic interference shielding performance, Nanoscale. 8 (2016) 16684–16693. https://doi.org/10.1039/C6NR02619B.

[12] X. Zhu, Y. Dong, Z. Xiang, L. Cai, F. Pan, X. Zhang, Z. Shi, W. Lu, Morphology-controllable synthesis of polyurethane-derived highly cross-linked 3D networks for multifunctional and efficient electromagnetic wave absorption, Carbon. 182 (2021) 254–264. https://doi.org/10.1016/j.carbon.2021.06.028.

[13] J. Zhang, M. Ma, Y. Bi, Z. Liao, Y. Ma, W. Huang, P. Lyu, C. Feng, A review of epoxy-based composite materials: Synthesis, structure and application for electromagnetic wave absorption, J. Alloys Compd. 922 (2022) 166096. https://doi.org/10.1016/j.jallcom.2022.166096.

[14] Z. Barani, F. Kargar, K. Godziszewski, A. Rehman, Y. Yashchyshyn, S. Rumyantsev, G. Cywiński, W. Knap, A.A. Balandin, Graphene Epoxy-Based Composites as Efficient Electromagnetic Absorbers in the Extremely High-Frequency Band, ACS Appl. Mater. Interfaces. (2020). https://doi.org/10.1021/acsami.0c06729.

[15] H. Breiss, A. El Assal, R. Benzerga, A. Sharaiha, A. Jrad, A. Harmouch, Ultra-porous and lightweight microwave absorber based on epoxy foam loaded with long carbon fibers, Mater. Res. Bull. 137 (2021) 111188. https://doi.org/10.1016/j.materresbull.2020.111188.

ACCEPTED MANUSCRIPT / CLEAN COPY

[16] R.-B. Yang, W.-F. Liang, S.-T. Choi, C.-K. Lin, The Effects of Size and Shape of Iron Particles on the Microwave Absorbing Properties of Composite Absorbers, IEEE Trans. Magn. 49 (2013) 4180–4183. https://doi.org/10.1109/TMAG.2013.2239973.
[17] F. Qin, C. Brosseau, A review and analysis of microwave absorption in polymer composites filled with carbonaceous particles, J. Appl. Phys. 111 (2012) 061301. https://doi.org/10.1063/1.3688435.
[18] C. Méjean, M. Badard, R. Benzerga, C. Le Paven-Thivet, A. Sharaiha, Rigid composite materials for anechoic chamber application, Mater. Res. Bull. 96 (2017) 94–99. https://doi.org/10.1016/j.materresbull.2017.01.023.
[19] C. Méjean, L. Pometcu, R. Benzerga, A. Sharaiha, C. Le Paven-Thivet, M. Badard, P. Pouliguen, Electromagnetic absorber composite made of carbon fibers loaded epoxy foam for anechoic chamber application, Mater. Sci. Eng. B. 220 (2017) 59–65. https://doi.org/10.1016/j.mseb.2017.03.009.
[20] Microwave absorbers, Siepel. (n.d.). https://www.siepel.com/en/microwave-absorbers/ (accessed October 23, 2023).
[21] C.-X. Yuan, Z.-X. Zhou, J.W. Zhang, X.-L. Xiang, Y. Feng, H.-G. Sun, Properties of Propagation of Electromagnetic Wave in a Multilayer Radar-Absorbing Structure With Plasma- and Radar-Absorbing Material, IEEE Trans. Plasma Sci. 39 (2011) 1768–1775. https://doi.org/10.1109/TPS.2011.2160285.
[22] A. El Assal, H. Breiss, R. Benzerga, A. Sharaiha, Design and optimization of ultra-wideband planar multilayer absorber based on long-carbon fiber-loaded composites, J. Mater. Sci. 56 (2021) 19484–19500. https://doi.org/10.1007/s10853-021-06453-5.
[23] H. Breiss, A. El Assal, R. Benzerga, C. Méjean, A. Sharaiha, Long Carbon Fibers for Microwave Absorption: Effect of Fiber Length on Absorption Frequency Band, Micromachines. 11 (2020) 1081. https://doi.org/10.3390/mi11121081.
[24] R. Benzerga, M. Badard, C. Méjean, A. El Assal, C. Le Paven, A. Sharaiha, Carbon Fibers Loaded Composites for Microwave Absorbing Application: Effect of Fiber Length and Dispersion Process on Dielectric Properties, J. Electron. Mater. 49 (2020) 2999–3008. https://doi.org/10.1007/s11664-020-07998-y.
[25] C.M. Watts, X. Liu, W.J. Padilla, Metamaterial Electromagnetic Wave Absorbers, Adv. Mater. 24 (2012). https://doi.org/10.1002/adma.201200674.
[26] Q. Huang, G. Wang, M. Zhou, J. Zheng, S. Tang, G. Ji, Metamaterial electromagnetic wave absorbers and devices: Design and 3D microarchitecture, J. Mater. Sci. Technol. 108 (2022) 90–101. https://doi.org/10.1016/j.jmst.2021.07.055.
[27] D.R. Smith, W.J. Padilla, D.C. Vier, S.C. Nemat-Nasser, S. Schultz, Composite Medium with Simultaneously Negative Permeability and Permittivity, Phys. Rev. Lett. 84 (2000) 4184–4187. https://doi.org/10.1103/PhysRevLett.84.4184.
[28] T. Hien Nguyen, S. Tung Bui, T. Tuan Nguyen, T. Tung Nguyen, Y. Lee, M. An Nguyen, D. Lam Vu, Metamaterial-based perfect absorber: polarization insensitivity and broadband, Adv. Nat. Sci. Nanosci. Nanotechnol. 5 (2014) 025013. https://doi.org/10.1088/2043-6262/5/2/025013.
[29] J. Sun, L. Liu, G. Dong, J. Zhou, An extremely broad band metamaterial absorber based on destructive interference, Opt. Express. 19 (2011) 21155. https://doi.org/10.1364/OE.19.021155.
[30] F. Ding, Y. Cui, X. Ge, Y. Jin, S. He, Ultra-broadband microwave metamaterial absorber, Appl. Phys. Lett. 100 (2012) 103506. https://doi.org/10.1063/1.3692178.

ACCEPTED MANUSCRIPT / CLEAN COPY

[31] T.Q.H. Nguyen, T.K.T. Nguyen, T.N. Cao, H. Nguyen, L.G. Bach, Numerical study of a broadband metamaterial absorber using a single split circle ring and lumped resistors for X-band applications, AIP Adv. 10 (2020) 035326. https://doi.org/10.1063/1.5143915.
[32] A. El Assal, H. Breiss, R. Benzerga, A. Sharaiha, A. Jrad, A. Harmouch, Toward an Ultra-Wideband Hybrid Metamaterial Based Microwave Absorber, Micromachines. 11 (2020) 930. https://doi.org/10.3390/mi11100930.
[33] Y.J. Yoo, J.S. Hwang, Y.P. Lee, Flexible perfect metamaterial absorbers for electromagnetic wave, J. Electromagn. Waves Appl. 31 (2017) 663–715. https://doi.org/10.1080/09205071.2017.1312557.
[34] Q. Zhou, X. Yin, F. Ye, X. Liu, L. Cheng, L. Zhang, A novel two-layer periodic stepped structure for effective broadband radar electromagnetic absorption, Mater. Des. 123 (2017) 46–53. https://doi.org/10.1016/j.matdes.2017.03.044.
[35] K.-L. Zhang, J.-Y. Zhang, Z.-L. Hou, S. Bi, Q.-L. Zhao, Multifunctional broadband microwave absorption of flexible graphene composites, Carbon. 141 (2019) 608–617. https://doi.org/10.1016/j.carbon.2018.10.024.
[36] F. Chen, H. Chai, Z. Song, L. Yu, C. Fang, Hydrophilic Porous Polydimethysiloxane Sponge as a Novel 3D Matrix Mimicking Heterogeneous Pores in Soil for Plant Cultivation, Polymers. 12 (2020) 140. https://doi.org/10.3390/polym12010140.
[37] D. Zhu, S. Handschuh-Wang, X. Zhou, Recent progress in fabrication and application of polydimethylsiloxane sponges, J. Mater. Chem. A. 5 (2017) 16467–16497. https://doi.org/10.1039/C7TA04577H.
[38] X. Zhang, W. Huo, Y. Lu, K. Gan, S. Yan, J. Liu, J. Yang, Porous Si3N4-based ceramics with uniform pore structure originated from single-shell hollow microspheres, J. Mater. Sci. 54 (2019) 4484–4494. https://doi.org/10.1007/s10853-018-3118-2.
[39] K.-L. Zhang, Z.-L. Hou, S. Bi, H.-M. Fang, Modeling for multi-resonant behavior of broadband metamaterial absorber with geometrical substrate, Chin. Phys. B. 26 (2017) 127802. https://doi.org/10.1088/1674-1056/26/12/127802.
[40] L. Pometcu, C. Méjean, R. Benzerga, A. Sharaiha, P. Pouliguen, C. Le Paven, On the choice of the dielectric characterization method for foam composite absorber material, Mater. Res. Bull. 96 (2017) 107–114. https://doi.org/10.1016/j.materresbull.2017.04.055.
[41] R.A. Fenner, E.J. Rothwell, L.L. Frasch, A comprehensive analysis of free-space and guided-wave techniques for extracting the permeability and permittivity of materials using reflection-only measurements, Radio Sci. 47 (2012). https://doi.org/10.1029/2011RS004755.

ACCEPTED MANUSCRIPT / CLEAN COPY

Graphical abstract

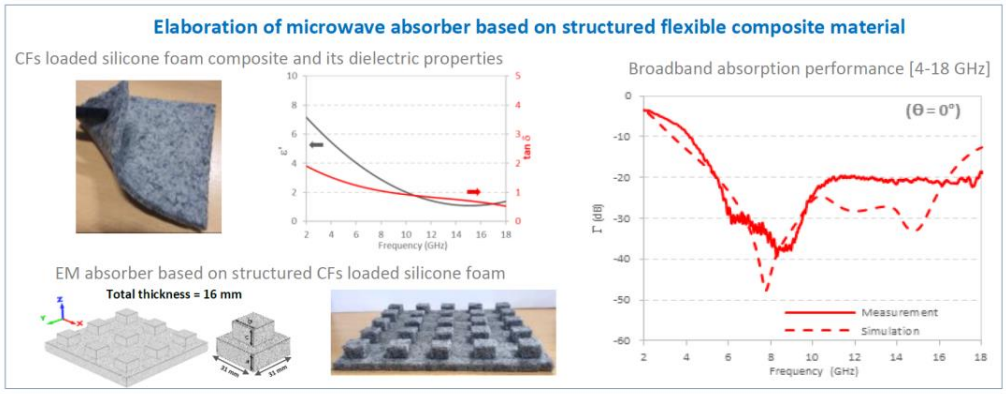

Declaration of competing interests

☒ The authors declare that they have no known competing financial interests or personal relationships that could have appeared to influence the work reported in this paper.

☐ The authors declare the following financial interests/personal relationships which may be considered as potential competing interests:

ACCEPTED MANUSCRIPT / CLEAN COPY